zero to 90 degrees. The insertion loss would be very sensitive to the mirror final (actuated) angle.

In order to stop the mirror and prevent electrical shorting, a special stopper is designed and positioned above the electrode. Because of the tilting angle from actuator and the bending of the stopper, the actuator will only contact the corner of the landing bar with a single point of contact. This is the key element to ensure high reliability and prevent stiction problems. It also helps to settle the mirror ringing and improve the switch time. The device can be driven by a square wave voltage function without pre-shaping waveform and still achieve 12 ms switching time. More than 100 million cycles have been demonstrated with repeatable mirror angle and performance. The actuator is moving in the air and not in contact with substrate except the single point contact of the final landing. It is different than sliding the mirror back and forth, which would make continuous mechanical contact with the surface.

3. Test Results

Figure 3 shows a SEM of 16 × 16 on single chip. Figure 4 shows the angle uniformity of <±0.1 degrees achieved with this technology. Collimators have been aligned to this chip and the component has been hermetically sealed before measuring performance parameters. For switches manufactured with this technology, the specified maximum insertion loss for a 16 × 16 is less than 6 dB for all states and cross-talk <–50 dB. Variation of loss over the entire 1280–1650 nm range is <1 dB. Return loss is >50 dB, and maximum temperature variation is <1 dB over a temperature range of 0–60 degrees C. Polarization Dependent Loss (PDL) is <0.4 dB and Polarization Mode Dispersion (PMD) is <0.08 ps. Maximum switch time is 12 ms. In fact, specific 16 × 16 switches have been manufactured with maximum insertion loss under 3.1 dB. Vibration tests showed <0.2 dB change under operation, and 3 axis shock tests confirm no change of operational characteristics under 200 G.

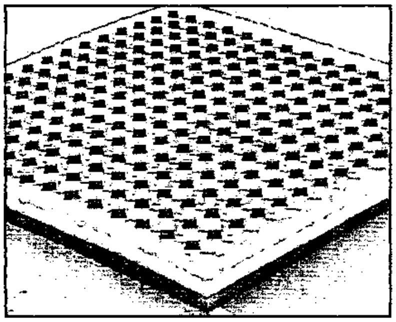

TuO4 Fig. 3. SEM of 16 × 16 array of 2D MEMS switch.

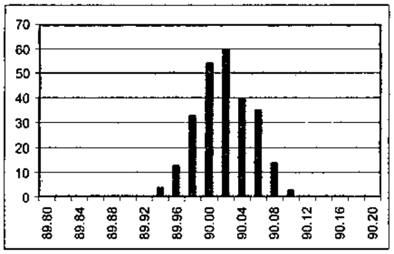

TuO4 Fig. 4. Angle histogram of mirror angles for typical 16 × 16 switch mirror.

4. Summary

In conclusion we have demonstrated fully nonblocking 16 × 16 switches in a single chip solution using MEMS fabricated by a surface micro-machining. We have shown how the critical mechanical elements of the MEMS-cell have been chosen to achieve large mechanical movement, high angular repeatability of the movement, and high reliability of the actuation mechanism, which translated into low loss and high reliability of the packaged component. Test results for these components have been presented.

References

1. H. Toshiyoshi, et al., J. MEMS, vol. 5, no. 4, pp. 231–237, 1996.
2. L.Y. Lin, et al., IEEE PTL, vol. 10, no. 4, pp. 525–527, 1998.
3. IEEE: A.Q. Liu, et al., LEOS, pp. 37–38, 2000.

TuO5 **3:15 pm**

Nano-Electro-Mechanical Photonic Crystal Switch

Ming-Chang Mark Lee, Dooyoung Hah, Erwin K. Lau, Ming Wu, *Department of Electrical Engineering, University of California at Los Angeles, Email: marklee@icsl.ucla.edu*

Hiroshi Toshiyoshi, *Institute of Industrial Science, University of Tokyo, Email: hiro@iis.u-tokyo.ac.jp*

1. Introduction

Photonic crystals (PCs) have the ability to confine light propagation within small volumes for specific frequency ranges, known as photonic bandgaps (PBG). Furthermore, by inserting defects in the host PBG structure, we can engineer high quality factors and narrow bandpass transmission spectra in the photonic bandgap. Due to these properties, many practical implement actions such as planar photonic crystal waveguides,[1–3] polarizers, optical filters,[4] optical switches and PBG defect mode lasers[5] were engineered. Potentially, integration of these passive and active elements can form complex optical circuits on a chip.

MEMS-based optical switches have been developed for optical networks in recent years, due to their capability to reduce insertion loss, crosstalk and power consumption.[6] A wide variety of device designs have been realized. Most switches either use micromirrors to change light path between input/output channels or directly move the waveguides or fibers for channel coupling.[7] In this paper, we demonstrate a 1 × 1 optical switch using an integrated photonic crystal with MEMS actuators.

2. Device Design

Photonic crystals can be classified as 1D, 2D, and even 3D structures, depending on how many dimensions the PC confines light. However, high dimension PC structures are still difficult to fabricate and are not easily integrated with actuators. In our design, an input and output Si waveguide are optically linked by a 1D PBG active component. We designed two separate PC structures: 1) a reflection state that serves as a broadband notch filter centered at 1.55 μm and extending from 1.0 μm to 2.1 μm 2) a transmission state with the same notch filter properties, however allowing a narrow bandpass at 1.55 μm. Connected to a MEMS actuator, the active component can be switched between either one of these structures. This allows us to control the flow of light as it passes along the waveguide. The whole structure is shown in Fig. 1a.

The reflection structure's silicon feature and air gaps were designed at quarter-wavelength thickness (from a 1.55 μm center wavelength). The transmission structure's silicon feature was designed at a full-wavelength thickness, allowing the peak transmittance located at the 1.55 μm center wavelength.[8]

The silicon was the material for the photonic crystal because of its high refractive index that enhances the Q of the filtering with only a few periods in compact periodic structure. The reflection state's silicon feature and air gaps were designed at quarter-wavelength thickness (from a 1.55 μm center wavelength). The transmission state's silicon feature was designed at a full-wavelength thickness, allowing the peak transmittance located at the 1.55 μm center wavelength.[8] The more detail dimension is shown in Fig. 1b.

2. Fabrication

The whole device was fabricated on a Silicon-On-Insulator (SOI) wafer. The thickness of device layer is 1.5 μm and the silicon dioxide layer is 0.5 μm. SOI was chosen due to its flat, monocrystalline surface and low residual stress of single crystal, which is more reliable for the nanofabrication. First, we grow 100 nm thermal oxide on the top of device. Then E-beam lithography and optical lithography was used to pattern structures. E-beam lithography combined with

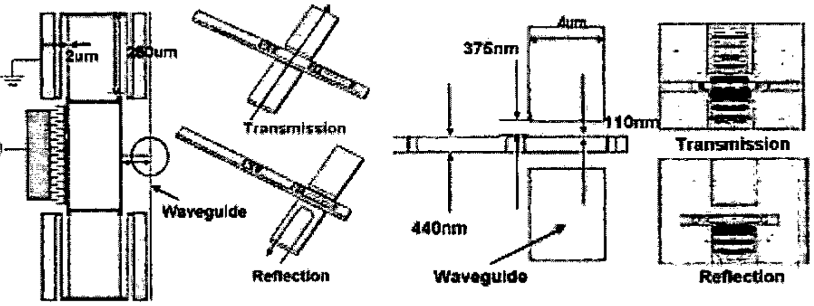

TuO5 Fig. 1. (a). Nano-Electro-Mechanical photonic crystal switch. The left hand part is the actuator. The right hand part is the 1D PBG active component with two different switch states. (b). Detail dimension of the optical component. The right hand part is FDTD simulation for different two state.

chrome evaporation and lift-off was applied to create the nano-scale PBG structures and waveguides. Optical lithography followed to create the microscale actuator parts. We used reactive ion etch (RIE) to etch the top silicon dioxide layer according to the pattern made by the E-beam/optical lithography. After photoresist was stripped, the silicon device layer was etched down by deep reactive ion etch (DRIE). Because the minimum feature is 110 nm, a precisely controlled anisotropy etch is needed.[9] Finally, we put the sample into hydrofluoric acid (HF) to etch the underside silicon dioxide and then use a supercritical dryer to release the structure. Fig. 2 is the SEM picture of fabrication result.

3. Experiment Result and Test

The device was tested using a 1.55 μm laser to couple light into the waveguide via a lensed fiber. At the receiver end, a CCD camera images the far field output waveguide pattern to help align input fiber to the waveguide. Another lensed fiber was then aligned to the output facet via photo detector. Once the I/O fibers were aligned to the waveguide, we replaced the infrared laser with a white light source and the photo detector with an optical spectrum analyzer. A 70 V DC voltage was applied to the actuator to let the reflection structure and the transmission structure change alternatively. The result is shown in Fig. 3. The transmittance of reflection structure and transmission structure was normalized to a straight waveguide without PBG. The peak transmittance was centered at 1.56 μm, which is close to our objective. An 11 dB extinction ratio was presented by comparing the transmittance of the reflection state and transmission state for 1.56 μm wavelength.

4. Conclusion

In this paper, we present the first electro-mechanical nanophotonic optical switch. A bi-state PBG structure was dynamically driven by a MEMS actuator to control the light propagation. An extinction ratio of 11 dB was demonstrated between the transmission state and reflection state for 1.56 μm wavelength.

Reference

1. Attila Mekis, J.C. Chen, I. Kurland, Shanhui Fan, Pierre R. Villeneuve and J.D. Joannopoulos, "High Transmission through Sharp Bends in Photonic Crystal Waveguides", Physical Review Letters, Vol. 77, No. 18, Oct. 1996, pp. 3787–90.
2. Marko Loncar, Dusan Nedeljkovic, Theodor Doll, Jelena Vuckovic, Axel Scherer and Thomas P. Pearsall, "Waveguiding in Planar Photonic Crystals", Applied Physics Letters, Vol. 77, No. 13, Sep. 2000, pp. 1937–39.
3. Marko Loncar, Theodor Doll, Jelena Vuckovic and Axel Scherer, "Design and Fabrication of Silicon Photonic Crystal Optical Waveguides", Journal of Lightwave Technology, Vol. 18, No. 10, Oct. 2000, pp. 1402–10.
4. J.S. Foresi, P.R. Villeneuve, J. Ferrera, E.R. Thoen, G. Steinmeyer, S. Fan, J.D. Joannopoulos, L.C. Kimerling, Henry I. Smith and E.P. Ippen, "Photonic-bandgap Microcavities in Optical Waveguides", Nature, Vol. 390, No. 13, Nov. 1997, pp. 143–45.
5. O. Painter, A. Husain, A. Schere, P.T. Lee, I. Kim, J.D. O'Brien and P.D. Dapkus, "Lithographic Tuning of a Two-Dimensional Photonic Crystal Laser Array", IEEE Photonics Technology Letters, Vol. 12, No. 9, Sep. 2000, pp. 1126–28.
6. Raanan A. Millar, Yu-Chong Tai, Guoda Xu, John Bartha and Freddie Lin, "An Electromagnetic MEMS 2 × 2 Fiber Optic Bypass Switch", Transducers '97, 1997 International Conference on Solid-State Sensors and Actuators, Chicago, June 16–19, 1997.
7. Shubin, I.; LiKamWa, P. "A guided-wave optical switch controlled by a micro-electromechanical cantilever", LEOS 2000. 2000 IEEE Annual Meeting Conference Proceedings, Piscataway, NJ, USA: IEEE, 2000. p. 50–1 vol. 1.
8. Pochi Yeh, "Matrix Formulation for Isotropic Layered Media" in *Optical Waves in Layered Media,* Joseph W. Goodman, Wiley Interscience.
9. Mikhail Naydenkov, Bahram Jalali, "Fabrication of High Aspect Ratio Photonic Bandgap Structures on Silicon-on-Insulater", Proceedings of the SPIE—The International Society for Optical Engineering, vol. 3936, (Integrated Optics Devices IV, San Jose, CA, USA, 24–25 Jan. 2000.) SPIE-Int. Soc. Opt. Eng, 2000. p. 33–9.

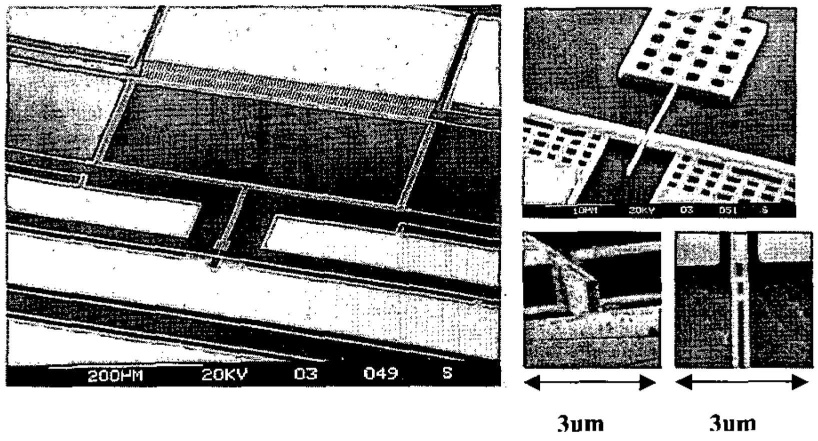

TuO5 Fig. 2. SEM picture of PBG switch.

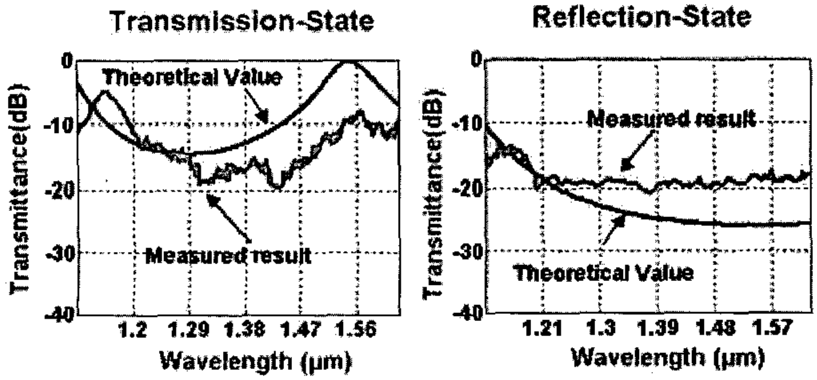

TuO5 Fig. 3. Testing result on transmittance. An 11 dB extinction ratio between the transmission state and reflection state for 1.56 μm wavelength.

TuO6 **3:30 pm**

Compliant MEMS and their Use in Optical Components

M. J. Little, CTO, *Solus Micro Technologies, 5706 Corsa Ave., Westlake Village, CA 91362*

Introduction

There has been a growing interest and excitement about MEMS technology (Micro-Electro-Mechanical Systems) since the introduction of the first commercial parts in the early 1990's. These early devices were mostly accelerometers used for triggering automobile air bags. In the subsequent years, there have been many other MEMS devices commercialized; most notably, the micromirror display device from Texas Instruments.[1] The past few years we have seen exciting descriptions of laboratory versions of MEMS devices for the optical communications industry. And now this year, we have seen several of these optical communications MEMS devices emerge from the laboratory into commercial availability; these include optical crossconnect switches, tunable lasers and tunable filters.

All of these traditional MEMS devices share a common heritage; their fabrication evolved from silicon processing technology. The deposition, patterning and etching required for fabricating MEMS uses the same equipment, processes and indeed the same materials as are used in the fabrication of integrated circuits.